Measuring quantitative proteomic distance between Spanish beef breeds

R. Rodríguez-Vázquez [a], A. Mato [a], M. López-Pedrouso [a], D. Franco [b], M. A. Sentandreu [c], C. Zapata [a,*]

[a]*Department of Zoology, Genetics and Physical Anthropology, University of Santiago de Compostela, 15782 Santiago de Compostela, Spain*

[b]*Meat Technology Center of Galicia, 32900 San Cibrao das Viñas, Ourense, Spain*

[c]*Instituto de Agroquímica y Tecnología de Alimentos (CSIC), 46980 Paterna, Valencia, Spain*

* Corresponding author at: Department of Zoology, Genetics and Physical Anthropology. University of Santiago de Compostela, 15782 Santiago de Compostela, Spain.

E-mail address: c.zapata@usc.es (C. Zapata).

Abstract

Estimates of quantitative proteomic distance between populations have not been reported to date. Here, quantitative proteomic distances between three Spanish bovine breeds (Asturiana de los Valles, AV; Retinta, RE; and Rubia Gallega, RG) were estimated from two-dimensional electrophoresis profiles of meat samples of *longissimus thoracis* muscle at 2 h *post-mortem*. Statistically significant distances were detected between AV/RG and the most genetically different RE breed, using the novel *QD* measure of quantitative proteomic distance. In total, 18 differentially abundant myofibrillar and sarcoplasmic proteins/isoforms contributing to proteomic distances between breeds were confidently identified by tandem mass spectrometry. The fast skeletal myosin regulatory light chain 2 followed by other five interacting proteins exhibited the most pronounced relative change between breeds. In addition, most differentially represented proteins could be associated with variations in meat tenderness. Therefore, they could be candidate biomarkers for molecular breeding programs and authentication of the three Spanish beef breeds.

Keywords: Meat proteomics, Population proteomics, Proteomic distance measures, QD measure, Beef tenderness biomarkers, Beef authenticity biomarkers

1. Introduction

A total of 1019 local cattle breeds have been recorded in the Global Databank for Animal Genetic Resources (FAO, 2015). Crossbreeding programs spanning decades of research have shown far-reaching differences between cattle breeds for carcass composition (e.g. fat thickness and carcass weight) and meat quality (e.g. tenderness) characteristics that are variably influenced by genetic make-up and environmental factors (Burrow, Moore, Johnston, Barendse, & Bindon, 2001). The application of high-throughput genomic technologies has provided valuable genome-wide data for thousands of markers, information about inter-breed genomic diversity and fueled the identification of quantitative trait loci (QTL) underlying inter-breed variations in carcass and beef quality attributes (Ramayo-Caldas, Renand, Ballester, Saintilan, & Rocha, 2016; Medeiros de Oliveira Silva et al., 2017).

Comparative proteomics can provide extremely valuable superimposed information to genetic studies to unraveling the complex molecular pathways and candidate QTL involved in meat quality variations between cattle breeds (Ohsaki et al., 2007; Timperio, D'Alessandro, Pariset, D'Amici, & Zolla, 2009; De Souza Rodrigues et al., 2017; Gagaoua, Terlouw, Richardson, Hocquette, & Picard, 2019). First of all, proteomics enables the analysis of the final products of the expression of protein coding genes involved in muscle-to-meat conversion as well as exploring genotype-environment crosstalk establishing a bridge between the genotype and the phenotype. Second, differential protein abundance in comparative proteomics is an alternative approach to positional QTL cloning to discover the candidate protein QTL (pQTL) underlying the trait of interest (Acharjee et al., 2018). Comparative proteomics between breeds has the added advantage that facilitates pQTL identification because the differences for carcass and meat quality attributes are significantly larger than within-

breed differences (Burrow et al., 2001). It also enables the discovery of breed-specific protein markers that can be used for meat authenticity and traceability throughout industrial production processes (Montowska & Pospiech, 2012; Fontanesi, 2017).

Proteomic distances can be a powerful tool for assessing summarized information on the degree of global proteomic divergence between populations. It must be highlighted, however, that the measurement of the proteomic distance is considerably more complex than the measurement of the genetic distance. In particular, the proteomic distance between a given pair of populations can undergo significant variations due to the enormous spatio-temporal plasticity of the proteome. To date, only a few studies have used proteomic distance measurements to assess the relationship of proteomic differentiation between populations with intraspecific phylogenetic diversity established by genetic markers in the parasite *Trypanosoma cruzi* (Telleria et al., 2010), genetic proximities between species and genus of the plant family Brassicaceae (Marquès, Sarazin, Chané-Favre, Zivy, & Thiellment, 2001), variations in quality traits in the common bean (*Phaseolus vulgaris*) and potato (*Solanum tuberosum*) (López Pedrouso, Bernal, Franco, & Zapata, 2014; Mouzo, López-Pedrouso, Bernal, García, Franco, & Zapata, 2018), and changes in beef tenderness (Gagaoua et al., 2019). Proteomic distances were assessed using Jaccard's and Nei and Li's distance measures (Jaccard, 1908; Nei & Li, 1979). These are proteomic distance measures of qualitative type, computed from the number of common and uncommon proteins between populations. Therefore, qualitative distances are useful when differences between proteomic profiles are qualitatively pronounced, exhibiting a large number of shared and unshared proteins. However, a more efficient and general measure of proteomic distance should also include quantitative differences in protein abundance. Measurements of distance computed from quantitative proteomic data have been traditionally used to assess the

level of similarity/dissimilarity between populations by multivariate statistical methods such as the principal component and cluster analyses. To the best of our knowledge, however, no estimates of the quantitative distance summarizing in a single numerical value the degree of proteomic divergence between populations have been reported to date.

In this study, quantitative proteomic distances between AV, RE and RG bovine breeds were assessed from two-dimensional electrophoresis (2-DE) proteomic profiles of *longissimus thoracis* (LT) muscle meats. These are the three major cattle breeds in the Spanish meat industry, accounting for ca. 78% of Spain's total beef production (MAPAMA, 2018). Proteomic distances between breed pairs were estimated by means of the recently proposed *QD* statistic that takes into account quantitative differential abundance of both shared and unshared proteins between populations (Rodríguez-Vázquez & Zapata, 2019). In addition, proteins contributing to proteomic distance between breeds were identified by MS/MS to gain deeper insights into the biochemical processes underlying distinctive meat characteristics and identify candidate protein markers for the authentication of the three Spanish beef breeds.

2. Materials and methods

2.1. Bovine breeds and meat samples

Three different bovine (*Bos taurus* L.) breeds raised in different Spanish regions were used in this study: AV (Asturias), RE (Extremadura) and RG (Galicia). Animals belonging to the three Spanish breeds were transported by road from farms to accredited abattoirs in a time not exceeding one hour and slaughtered following the requirements established by European Union legislation (Council Directive 93/119/EEC) without further carcass intervention. Male calves of the three breeds were slaughtered at the usual age in the Spanish beef industry: 9-10 months in the AV and RE breeds and 5-6

124 months in the RG cattle breed. Meat samples from each cattle breed were collected at 2
125 h post-mortem to avoid proteomic differences caused by post-mortem meat processing
126 variations among slaughterhouses. One steak of 2 cm was excised from each animal at
127 the thirteenth rib position of the LT muscle. Meat samples were vacuum packed,
128 transported to the laboratory under refrigerated conditions, lyophilized and stored at -80
129 ^{o}C. Six independent biological replicates of each of the three breeds were used for
130 proteomic analyses.

131 *2.2. Protein extraction and quantification*

132 Total protein was extracted from lyophilized meat samples as described by
133 Franco et al. (2015). An amount of 50 mg of each lyophilized sample was mixed with
134 1.5 mL of lysis buffer (7 M urea; 2 M thiourea; 10 mM dithiothreitol, DTT; 4%
135 CHAPS; and 2% Pharmalyte^{TM} pH 3-10, GE Healthcare, Chicago) and subjected to
136 sonication (Sonifier 250, Branson, Danbury) in an ice-water bath. The proteins were
137 purified using the Clean-Up Kit (GE Healthcare) and resuspended in 500 µL of lysis
138 buffer. Quantitation of the total protein concentration was performed with the CB-X
139 protein assay kit (G-Biosciences, St. Louis) based on an improved Bradford method,
140 using a Chromate 4300 (Awareness Technology, Palm City) microplate reader. Bovine
141 serum albumin (BSA) was used as protein standard for calibration.

142 *2.3. Two-Dimensional Electrophoresis*

143 LT muscle proteins were separated by previously established 2-DE protocols
144 (Franco et al., 2015). Briefly, 450 µg of total protein extract were dissolved in lysis and
145 rehydration (7 M urea, 2 M thiourea, 4% CHAPS, 0,002% bromophenol) buffers along
146 with 0.6% DTT and 1% immobilized pH gradient (IPG) buffer (Bio-Rad Laboratories,
147 Hercules). The mixture was loaded onto 24-cm-long IPG strips with linear pH gradient
148 of 4-7 (Bio-Rad Laboratories). First dimensional isoelectric focusing (IEF) was

performed using a PROTEAN IEF cell system (Bio-Rad Laboratories) applying an increasing voltage until reaching 70 kVh after an initial rehydration step (50 V for 12 h). Focused strips were equilibrated with equilibration buffers I (50 mM Tris pH 8.8; 6 M urea; 1% DTT; 30% glycerol; and 2% sodium dodecyl sulphate, SDS) and II (50 mM Tris pH 8.8, 6 M urea, 30% glycerol; 2% SDS; and 2.5% iodoacetamide) for 15 min each at room temperature. SDS-polyacrilamide gel electrophoresis (SDS-PAGE) for the second dimension was performed by transferring strips to 13% (w/v) gels of 24 × 20 cm and run on an Ettan DALTsix vertical multigel electrophoresis system (GE, Healthcare) at 18 mA/gel for 15 h after an initial step of 6 mA/gel for 1 h. Gels were subsequently stained with SYPRO Ruby fluorescent stain (Lonza, Rockland) following the manufacturer's indications. Protein molecular mass markers between 15 to 200 kDa (Fermentas, Ontario) were loaded into a lateral well of SDS-PAGE gels.

2.4. Image analysis

The 2-DE gels were scanned using a Gel Doc XR + system (Bio-Rad Laboratories). Detection, matching and volume quantitation of spots was automatically performed with PDQuest Advanced software v. 8.0.1 (Bio-Rad Laboratories) and manually checked. Normalized volumes of the spots were obtained after background subtraction using the total density of validated spots across all replicate gels. Only spots reproducibly validated in at least four replicates of each cattle breed were considered for further analyses. The isoelectric point (p*I*) and molecular weight (M_r) of each spot were obtained using as a reference the above-mentioned linear IPG strips (pH 4-7) and standard molecular mass markers, respectively.

2.5. Protein identification by mass spectrometry

Protein identification was accomplished by MALDI-TOF and MALDI-TOF/TOF MS as previously (Franco et al., 2015). Briefly, spots of interest were excised

from gels and submitted to in-gel trypsin digestion. Eluted peptides were concentrated in a SpeedVac (Thermo Fisher Scientific, Waltham) and stored at -20 ºC until mass spectrometric analysis. A mixture of peptides redissolved in formic acid and matrix solution was transferred onto a 384 well Opti-TOF MALDI target plate (Applied Biosystems, Foster City) using the thin layer method. Mass spectra were then recorded on a 4800 MALDI-TOF/TOF mass spectrometer (Applied Biosystems) in the positive-ion reflector mode, an Nd:YAG laser with wavelength of 355 nm and an average of 1000 laser shots/spectrum. Mass calibration was performed using at least three trypsin autolysis peaks. Precursor ions for subsequent MS/MS fragment analysis were selected with a relative resolution of 300 full width at half-maximum (FWHM) and metastable suppression. The 4000 Series Explorer Software v. 3.5 (Applied Biosystems) was used to create an automated analyses of mass data. Search of peptide mass fingerprinting (PMF) and MSMS fragment-ion spectra data against the *B. taurus* UniProtKB/SwissProt non-redundant protein database was carried out through the GPS Explorer Software v. 3.6 using Mascot software v. 2.1 (Matrix Science, Boston), taking into account the following settings: a precursor and fragment ion mass tolerance of 30 ppm and 0.35 Da, respectively; the carbamidomethyl-Cys (CAM) and the oxidized methionine as fixed and variable modifications, respectively; and one missed cleavage allowed. Identifications by Mascot were manually validated. Protein identifications required at least three peptide matches to the same protein and Mascot's *P*-value < 0.05 significance threshold.

2.6. Statistical analysis

Non-parametric bootstrap was used to obtain confidence intervals (CIs) for the means of spot volumes across replicates of each breed according to Franco et al. (2015). For each spot, 20000 bootstrap samples of size *n* (number of replicates = 6) were drawn

with replacement using a Monte Carlo algorithm. The bootstrapped 95% CI were constructed from a distribution of 20000 mean replications by the bias-corrected percentile method (Efron, 1982). Bootstrap CIs were corrected for multiple comparisons with the Bonferroni method to make the familywide error rate α equal to 0.05. CIs were calculated using open-source R statistical software.

Quantitative changes of spot volumes between pairs of breeds were assessed by the fold change (*FC*) and relative change (*RC*) measures (Franco et al., 2015). The measure *FC* between pairs of breeds was calculated by $FC_{AV\text{-}RE} = V_{RE}/V_{AV}$, $FC_{AV\text{-}RG} = V_{RG}/V_{AV}$, $FC_{RE\text{-}RG} = V_{RG}/V_{RE}$, where V_{AV}, V_{RE} and V_{RG} are the mean volumes of the same spot on 2-DE gels from six replicate samples of the AV, RE and RG breeds, respectively. *FC*-values less than one were represented by their reciprocals with a negative sign. Therefore, *FC* ranges from -∞ to +∞. The *RC* measure is given by $RC = DV/|DV_{max}|$ where DV is the differential volume of a given spot between pairs of breeds: $DV_{AV\text{-}RE} = V_{RE} - V_{AV}$, $DV_{AV\text{-}RG} = V_{RG} - V_{AV}$ and $DV_{RE\text{-}RG} = V_{RG} - V_{RE}$; and where DV_{max} is the maximum observed value of DV (in absolute value) across all pairwise comparisons. The range of *RC* varies between -1.0 and +1.0.

The relationship between samples from standardized spot volume data (mean of 0 and standard deviation of 1) was assessed with a principal component analysis (PCA) and the generation of the heatmap using XLSTAT software (v. 2014.5.03; Addinsoft, Andernach). An UPGMA (Unweighted Pair Group with Arithmetic Mean) dendrogram was generated to cluster the proteins with significant differential ($P < 0.05$) abundance between breeds from the matrix of *RC*-values in absolute value using XLSTAT software. Descriptive statistics were calculated using IBM SPSS Statistics software (v.24; SPSS, Chicago).

2.7. Proteomic distance measures

Qualitative proteomic distances between pairs of breeds were estimated using Nei and Li's and Jaccard's distance indexes (Nei et al., 1979; Jaccard, 1908). Nei and Li's dissimilarity index is given by $D = 1 - F$; where $F = 2n_{xy} / (n_x + n_y)$, n_{xy} is the total number of spots shared between bovine breeds *x* and *y*, and where n_x and n_y are the total number of spots in breeds *x* and *y*, respectively. Jaccard's dissimilarity index becomes $D = 1 - J$, where $J = n_{xy} / (n_{xy} + a + b)$, and where *a* and *b* are unique spots only represented in breeds *x* and *y*, respectively. Quantitative changes in protein abundance between each pair of breeds were assessed using the *QD* measure of proteomic distance (Rodríguez-Vázquez et al., 2019), given by

$$QD = \left(\sum_{i=1}^{N} \left| RC_i \right| \Big/ N \right) p$$

where RC_i are the values of *RC* across *N* spots with statistically significant differential abundance between each pair of breeds and where *p* is the proportion of significantly changing spots. Therefore, *QD* ranges from 0 to 1.0. Non-parametric bootstrap was used to construct 95% CIs for qualitative and quantitative proteomic distance measures by the bias-corrected percentile method adjusted with the Bonferroni method from 20000 bootstrap resamples.

2.8. Bioinformatic analysis

Functional categorization of differentially abundant proteins between breeds in the three different ontologies (i.e. biological process, cellular component and molecular function of gene products) was performed from high levels of Gene Ontology (GO) slim terms using the Slimmer tool of AmiGO software (Carbon et al., 2009). The QuickGO web-based tool (Binns, Dimmer, Huntley, Barrell, O'Donovan, & Apweiler, 2009) was used for fine-grained information about each significantly changing protein between breeds. GO term enrichment analysis and over-representation of GO terms against the rest of the genome of *B. taurus* in KEGG and Interpro databases was performed with

249 the FatiGO/Babelomics software (Alonso et al., 2015). Significant over-representation
250 of GO terms was tested by means of the two-tailed Fisher exact test and global cut-off
251 value for multiple testing was established by the false discovery rate (FDR) procedure.

252 The search for known and predicted networks of direct protein-protein
253 interactions between differentially abundant proteins between breeds and interacting
254 partners in the proteome of *B. taurus* was carried out using the STRING v11.0 protein-
255 protein interaction database (Szklarczyk et al., 2019).

256 **3. Results**

257 *3.1. Comparison of 2-DE profiles between bovine breeds*

258 Representative 2-DE protein profiles for LT meat samples of each Spanish
259 bovine breed (AV, RE and RG) are shown in Fig. 1. The detection, matching and
260 volume measurement of 2-DE gel spots throughout six biological replicates of each
261 breed was carried out using the PDQuest software. A total of 140 individual protein
262 spots were matched across replicated gels of the three breeds. Mean volumes (± SE,
263 standard error) with their 95% bootstrap CIs for significantly changing protein spots
264 between pairs of breeds are shown in Supplementary Table 1. These spots were
265 numbered and marked on 2-DE gels (Fig. 1). Overall, 26.4% (37 out of 140) of spots
266 exhibited significant differential abundance between one or more pairs of breeds. A
267 Venn diagram was generated to show the number of these 37 differentially represented
268 protein spots that are shared and unshared by the three breeds (Supplementary Fig. 1). A
269 total of 17 (45.9%) and 1-5 (2.7-13.5%) spots coincided among the three breeds and
270 between pairs of breeds, respectively. Five unshared or unique spots were detected in
271 both AV (spots 5, 19, 20, 28 and 35) and RE (spots 4, 6, 14, 24 and 26), while unique
272 spots were no identified in the RG breed.

The principal component analysis (PCA) ordination method and heat map clustering were used to obtain summarized information about the relationships between the 37 protein spots with significant differential ($P < 0.05$) abundance between breeds. The two-dimensional PCA-plot shows that the first two principal components account for over 63% of the total variation in the data (Supplementary Fig. 2). The first principal component (41% of the total variation) clearly differentiated the samples into three well-separated clusters that correspond to the three breeds. Heat map clustering revealed that protein abundance was quite heterogeneous over spots of different breeds compared to spots of the same breed (upper dendrogram, Fig. 2). In addition, meat samples were divided into the same three clusters reflected in the PCA (left dendrogram, Fig. 2). The most separated cluster corresponded to RE meat samples, while clusters of AV and RG samples were closer to each other. These results indicate that 2-DE proteome profiles allowed the successfully allocation of each meat sample to the breed of origin.

3.2. Identification of differentially changing proteins

In total, 25 out of 37 differentially abundant protein spots between pairs of breeds were confidently ($P < 0.05$) identified by MALDI-TOF and MALDI-TOF/TOF MS (Table 1). The comparison between the theoretical (Th) and observed (Obs) M_r of each protein was used to exclude degraded proteins from further analysis. We considered that proteins were degraded when the ratio M_r (Th)/M_r (Obs) > 1.5, as previously (López-Pedrouso et al., 2018). A total of 7 proteins identified fulfil this criterion: EOGT (spot 14); FAM110A (spot 32); DUSP11 (spot 33); FAM110A-1 (spot 34); ATXN10 (spot 35); BCAT2 (spot 36); and SCKA1 (spot 37). Consequently, 18 protein spots and 12 non-redundant proteins differentially represented in bovine meat samples were eventually selected and used hereafter in further analyses: MYBPH (spot 1), MYBPH-1 (spot 3), CKM (spot 9), PRDX3 (spot 11), PRDX3-1 (spot 26), ACTA1

298 (spot 12), ACTA1-1 (spot 18), PDHB (spot 13), PDHB-1 (spot 16), TNNT1 (spot 17),
299 ANK2 (spot 19), YWHAE (spot 21), CCNG1 (spot 22), MYL6B (spot 25), TMEM233
300 (spot 27), MYLPF (spot 29), MYLPF-1 (spot 30) and MYLPF-2 (spot 31).

301 *3.3. Quantitation of the extent of change in protein abundance between breeds*

302 Changes of differentially ($P < 0.05$) abundant proteins between breeds estimated
303 by *FC* and *RC* measures are shown in Supplementary Table 2. It can be seen that *RC*
304 provides a more efficient overall estimation of the extent of change in protein
305 abundance between breeds than the traditionally used *FC* measure. The *FC* measure
306 gives values of -∞ or +∞ for unshared or unique protein spots regardless of the
307 differences in volume between breeds. In contrast, *RC* is a measure that ranges from -
308 1.0 to +1.0 and quantifies the existing differential abundance across both shared and
309 unshared proteins (Franco et al., 2015; López-Pedrouso et al., 2018; Mato, Rodríguez-
310 Vázquez, López-Pedrouso, Bravo, Franco, & Zapata, 2019). Note that *RC*-estimates (in
311 absolute value) across pairwise comparisons with *FC*-values of -∞ or +∞ in the present
312 study ranged from 0.008 to 0.081 and averaged (± SE) 0.023 ± 0.004 (Supplementary
313 Table 2).

314 Estimates of *RC* between breeds disclosed several outstanding facts. First,
315 changes in protein abundance were higher in pairwise comparisons including the RE
316 breed. Thus, the mean (± SE) of *RC*-values between AV-RE and RE-RG breeds was
317 0.169 ± 0.099 and 0.175 ± 0.088, respectively, whereas for AV-RG breeds the mean
318 decreased remarkably to 0.026 ± 0.006. These differences in *RC* mean values were
319 statistically significant using 95% bootstrap CIs obtained by the bias-corrected
320 percentile method. Secondly, MYLPF and MYLPF-2 were the proteins with the most
321 pronounced differential abundance between AV-RE (*RC* = +1.0) and RE-RG breeds
322 (*RC* = +0.495), respectively, whereas between AV-RG breeds was the CKM protein

(*RC* = -0.054). Accordingly, the UPGMA cluster analysis showed that MYLPF/MYLPF-2, MYLPF and CKM proteins formed separated subclusters in AV/RE, RE/RG and AV/RG dendrograms, respectively, constructed from the matrix of pairwise differences between *RC*s in absolute value (Fig. 3).

3.4. Bioinformatic analysis of identified proteins

The map of granular annotations and fine-grained information for the 12 differentially ($P < 0.05$) abundant proteins between breeds from GO terms retrieved through AmiGO and QuickGO tools are shown in Supplementary Fig. 3 and Supplementary Table 3, respectively. Proteins were involved in three ontology categories: i) cellular component (e.g. nucleus, cytoskeleton, extracellular space and myosin and troponin complexes); ii) molecular function (e.g. calcium ion binding, apoptotic process and catalytic activity); and iii) biological process (e. g. regulation of cell cycle, sarcomere organization and skeletal muscle development and assembly). No statistically significant over-representation of GO terms against the rest of the genome of *B. taurus* was detected from KEGG and Interpro databases following term enrichment analysis with the FatiGO/Babelomics software.

The protein-protein interaction map for the 12 differentially abundant proteins in AV, RE and RG breeds according to the STRING database is shown in Fig. 4. The resulting STRING map disclosed a single protein-protein interaction network that includes 6 out of 12 changing proteins. Interacting proteins are myofibrillar proteins involved in muscle structure-contraction (MYLPF, MYL6B, MYBPH, ACTA1), regulation of muscle contraction (TNNT1) and energy metabolism (CKM). It is noteworthy that MYLPF is the only node interacting with the rest of proteins of the interaction network.

3.5. Proteomic distance between breeds

Qualitative and quantitative proteomic distances between pairs of breeds are shown in Fig. 5 and Supplementary Table 4. Qualitative distances estimated by Nei and Li's *D* measure were lower that those distances estimated by Jaccard's *D* measure. It can be mathematically proven that both measurements report the same distance value only if all spots are either shared (n_{xy} = 1; *D* = 0) or unshared (n_{xy} = 0, *D* = 1); otherwise ($n_{xy} \neq 1$ and 0), Nei and Li's *D* scores are always lower than those of Jaccard's *D* measure. Overall, qualitative distances between AV-RE and RE-RG breeds were slightly higher than between AV-RG breeds, but not statistically different from each other. In contrast, statistically significant proteomic differentiation between breed pairs was detected by using the *QD* measure of quantitative proteomic distance (Fig. 5 and Supplementary Table 4). More specifically, quantitative distances were very similar between AV-RE (*QD* = 0.0145) and RE-RG (*QD* = 0.0142) breeds ($P > 0.05$), but about ten times higher than between AV-RG (*QD* = 0.0014) breeds ($P < 0.05$).

4. Discussion

Estimates of qualitative and quantitative proteomic distances calculated from 2-DE profiles of meat samples from LT muscle provided opposite information about the overall proteomic differentiation between Spanish bovine breeds. Proteomic distance between breeds was statistically validated only from quantitative differences in protein abundance. For this purpose, we used the *QD* measure specifically tailored to estimate distances between populations from quantitative proteomic data. Several lines of evidence support the satisfactory behavior of the *QD* statistic for measuring quantitative distances between populations. First of all, our observations indicate that the overall proteomic profiles of AV and RG meats were noticeably differentiated ($QD_{\text{AV-RG}}$ = 0.0014) from RE meat ($QD_{\text{AV-RE}}$ = 0.0145; $QD_{\text{RE-RG}}$ = 0.0142; $P < 0.05$). There results are consistent with the heat map clustering analysis based on differentially ($P < 0.05$)

represented proteins, showing that AV y RG breeds are grouped into two close sub-clusters clearly separated from the RE breed. Likewise, the hierarchical neighbour-joining (NJ) tree for 40 Iberian Peninsula cattle breeds using kinship distances computed from microsatellite marker data showed that AV is more closely related to RG than to RE (Cañón et al., 2011). This latter result is in agreement with genetic distance estimates between the three Spanish cattle breeds using the bovine high-density single-nucleotide polymorphism (SNP) chip (Cañas-Álvarez et al., 2015). More specifically, reported values of Nei's *D* genetic distance were lower between AV-RG breeds (*D* = 0.0095) than between RE and both AV and RG breeds (*D* = 0.0109-0.0137).

A total of 18 differentially abundant 2-DE protein spots containing 12 non-redundant myofibrillar and sarcoplasmic proteins, with a variable number of isoforms (zero to three), contributed to explaining proteomic distances between Spanish breeds. Proteins identified are involved in structural-contractile (MYBPH, ACTA1, ANK2, TNNT1, MYL6B and MYLPF), metabolism (CKM, PRDX3, PDHB and YWHAE), regulation of cell cycle (CCNG1) and nervous system development (TMEM233) related functions. Some of them might be candidate proteins involved in the existing differences between the three breeds for meat tenderness. Meat tenderness from the LT muscle of male calves of the three breeds was previously evaluated using the Warner-Bratzler shear force (WBSF) test (López-Pedrouso et al., 2019). The results of the WBSF test revealed statistically significant differences ($P < 0.001$) in tenderness between all pairs of sample groups. More specifically, RE and RG beefs were the least and most tender, respectively, while that of AV took intermediate tenderness scores.

MYLPF and interacting proteins can play a key role in causing differences in tenderness between the three Spanish cattle breeds. Thus, isoforms of MYLPF (i.e.

MYLPF, MYLPF-1 and MYLPF-2) were the proteins with the most pronounced relative change in protein abundance between RE and AV/RG meats (absolute values of *RC* ranged from 0.30 to 1.0). In contrast, no differential abundance of MYLPF isoforms was detected between AV and RG meats. MYLPF is a phosphoprotein with levels of phosphorylation modulated by the concerted action of Ca2+/calmodulin-dependent skeletal muscle myosin light chain kinase and protein phosphatase type 1 activities (Stull, Kamm, & Vandenboom, 2011). A number of studies in bovine, ovine and porcine have shown that changes in MYLPF phosphorylation levels are related to phenomena with impact in meat tenderness such as the skeletal muscle contraction force of fast-twitch fibers type IIb, the progress of *rigor mortis*, the response to pre-slaughter stress, actomyosin dissociation and myosin degradation (Muroya, Ohnishi-Kameyama, Oe, Nakajima, Shibata, & Chikuni, 2007; Franco et al., 2015; Chen et al., 2016; Lana & Zolla, 2016; Cao, Hou, Shen, Zhang, & Wang, 2019; Mato et al., 2019). In addition, we found that MYLPF is the single protein interacting with all partners (i.e. MYBPH, ACTA1; MYL6B, TNNT1 and CKM) of the protein-protein interaction network identified in our study. Changes in abundance/phosphorylation of all these interacting proteins have been consistently related to meat tenderness variations (Franco et al., 2015; Lana et al., 2016; Mato et al., 2019; Picard & Gagaoua, 2010). Differential abundance/phosphorylation of MYLPF (or other MYL2 isoforms), MYBPH, TNNT1, and CKM, between meat samples of *longissimus* muscle from different cattle breeds (Japanese Black vs. Holstein; Angus vs. Nellore; and Blond d'Aquitaine vs. Charolais and Limousin) have been previously reported (Ohsaki et al., 2007; Chaze et al., 2013; de Souza Rodrigues et al., 2017). Overall, our study suggests that MYLPF isoforms and the network of interacting proteins constitute the main candidate markers of beef tenderness variations in the three Spanish bovine breeds.

Another subset of differentially abundant proteins in the three Spanish breeds (i.e. ANK2, PRDX3, PDHB, YWHAE, CCNG1 and TMEM233) did not show protein-protein interactions according to STRING database. Several of these proteins have been related to a number of beef quality traits, including tenderness and water holding capacity. Thus, ANK2 is a member of a family of structural proteins linking the integral membrane proteins to the underlying spectrin-actin cytoskeleton in a complex network of inter-myofibril and myofibril-sarcolemma connections that can be degraded by calpains, thus leading to meat tenderization (Aslan, Sweeney, Mullen, & Hamill, 2010). Polymorphisms in the bovine ANK1 have been associated with tenderness and intramuscular fat content, while in pork have bean associated with shear force, water-binding capacity, drip loss and other parameters related to meat-quality traits (Wimmers et al., 2007; Aslan et al., 2010). In accordance with this evidence, the ANK2 protein was identified only in more tender meat from AV and RG breeds. The PRDX·3 belongs to a ubiquitous family of cysteine-based peroxidases with a protective antioxidant function (Perkins, Nelson, Parsonage, Poole, & Karplus, 2015). Another peroxiredoxin, PRDX6, is considered to be a good marker of beef tenderness due to its anti-apoptotic properties (Gagaoua et al., 2019). The precursor protein of PRDX3 was recently associated with tender meat samples in Norwegian Red cattle (Graběz et al., 2015). Interestingly, we also found that the PRDX3 precursor protein (spot 11) was only identified in more tender meat of the AV and RG breeds. However, the active form of PRDX3 (PRDX3-1, spot 26) was only identified in less tender meat of RE cattle, the same negative relationship with tenderization that the PRDX6 peroxiredoxin. Finally, YWHAE belongs to the 14-3-3 protein family that binds to functionally diverse signaling proteins (Fu, Subramanian, & Masters, 2000). It was proposed that YWHAE phosphorylation might be involved in beef tenderness by preventing apoptosis and

448 increasing muscle contraction force (de Souza Rodrigues et al., 2017). However,
449 YWHAE was only identified in more tender meat of AV and RG breeds, which
450 suggests that it might be the unphosphorylated isoform of the protein.

451 The detection of breed-specific protein markers is useful for the authentication
452 of the origin of the meat to guarantee food quality and safety (Fontanesi, 2017). PCA
453 and heat map analyses disclosed that individual meats of each of the three Spanish
454 breeds can be distinguished unambiguously from global 2-DE proteome profiles. Single
455 proteins with changes in abundance between the three breeds could also be used for
456 meat authenticity. In particular, MYLPF isoforms would be good candidate markers for
457 this purpose because they underwent the most pronounced quantitative change between
458 breeds. It has been reported that the combination of different isoforms of the myosin
459 light chain enables differentiation between beef, pork and poultry due to the low
460 susceptibility of these isoforms to proteolytic degradation (Sentandreu, Fraser, Halket,
461 Patel, & Bramley, 2010; Montowska & Pospiech, 2012). Overall, candidate protein
462 identification for meat authentication could be routinely performed from muscle extracts
463 using faster and simple alternative analytical methods, including immunoassay
464 techniques. Further follow-up research is needed to establish whether these protein
465 markers can be applied for beef authentication and traceability in a wider range of
466 scenarios, including different breeds, muscles and beef aging.

467 **5. Conclusions**

468 This study leads us to conclude that the measurement of quantitative proteomic
469 distance is a valuable approach for the assessment of the degree of overall divergence of
470 the functional genome between populations, the sub-proteome linked to their variations
471 in biological traits and protein markers of populations. Comparative analysis between
472 qualitative and quantitative distance measures also showed that quantitative distances

provide more reliable information on the extent of proteomic differentiation between populations. Most of the 18 myofibrillar and sarcoplasmic proteins/isoforms with statistically significant differential abundance between the three Spanish breeds studied are functionally related to variations in meat tenderness. Therefore, they could be candidate pQTL in molecular breeding for meat quality improvement. Between-breed differentially represented proteins could also be useful markers to reduce the risk of mislabelling and frauds involving these Spanish beef breeds with Protected Denomination of Origin. Overall, our results suggest new avenues for research and practical applications in population proteomics, including the assessment of the relative efficiency of gel-based and gel-free driven proteomic studies in the estimation of proteomic distance, spatio-temporal variations in proteomic distance and the relationship between proteomic distance and the differentiation underlying biological traits.

Declaration of Competing Interest

The authors declare that they have no known competing financial interests or personal relationships that could have appeared to influence the work reported in this paper.

Acknowledgments

The authors would like to thank the anonymous reviewers for their valuable comments and suggestions to improve the quality of the article. This work was supported by the Instituto Nacional de Investigación y Tecnología Agraria (INIA, RTA 2014-00034-C04), Spain; and by a predoctoral fellowship of the Xunta de Galicia (Spain) and the European Union (ESF) to R. Rodríguez-Vázquez.

Appendix A. Supplementary data

Supplementary data to this article can be found online at……..

References

Acharjee, A., Chibon, P.-Y., Kloosterman, B., America, T., Renault, J., Maliepaard, C., & Visser, R. G. F. (2018). Genetic genomics of quality related traits in potato tubers using proteomics. *BMC Plant Biology*, *18*, 1-10.

Alonso, R., Salavert, F., Garcia-Garcia, F., Carbonell-Caballero, J., Bleda, M., Garcia-Alonso, L., Sanchis-Juan, A., Perez-Gil, D., Marin-Garcia, P., Sanchez, R., Cubuk, C., Hidalgo, M. R., Amadoz, A., Hernansaiz-Ballesteros, R. D., Alemán, A., Tarraga, J., Montaner, D., Medina, I., & Dopazo, J. (2015). Babelomics 5.0: functional interpretation for new generations of genomic data. *Nucleic Acids Research*, *43*, W117-W121.

Aslan, O., Sweeney T., Mullen, A. M., & Hamill, R. M. (2010). Regulatory polymorphisms in the bovine *Ankyrin 1* gene promoter are associated with tenderness and intramuscular fat content. *BMC Genetics*, *11*, 111.

Binns, D., Dimmer, E., Huntley, R., Barrell, D., O'Donovan, C., & Apweiler, R. (2009). QuikGo: a web-based tool for Gene Ontology searching. *Bioinformatics*, *25*, 3045-3046.

Burrow, H. M., Moore, S. S., Johnston, D. J., Barendse, W., & Bindon, B. M. (2001). Quantitative and molecular genetic influences on properties of beef: a review. *Australian Journal of Experimental Agriculture*, *41*, 893-919.

Cañas-Álvarez, J. J., González-Rodríguez, A., Munilla, S., Varona, L., Díaz, C., Baro, J. A., Altarriba, J., Molina, A., & Piedrafita, J. (2015). Genetic diversity and divergence among Spanish beef cattle breeds assessed by a bovine high-density SNP chip. *Journal of Animal Science*, *93*, 5164-5174.

Cañón, J., García, D., Delgado, J. V., Dunner, S., Da Gama, L. T., Landi, V., Martín-Burriel, I., Martínez, A., Penedo, C., Rodellar, C., Zaragoza, P., & Ginja, C.

(2011). Relative breed contributions to neutral genetic diversity of a comprehensive representation of Iberian native cattle. *Animal, 5*, 1323-1334.

Cao, L., Hou, C., Shen, Q., Zhang, D., & Wang, Z. (2019). Phosphorylation of myosin regulatory chain affects actomyosin dissociation and myosin degradation. *International Journal of Food Science and Technology, 54*, 2246-2255.

Carbon, S., Ireland, A., Mungall, C. J., Shu, S. Q., Marshall, B., Lewis S., the AmiGo Hub, & the Web Presence Working Group. (2009). AmiGO: online access to ontology and annotation data. *Bioinformatics, 2*, 288-289.

Chaze, T., Hocquette, J.-F., Meunier, G., Renand, G., Jurie, C., Chambon, C., Journaux, L., Rousset, S., Denoyelle, C., Lepetit, J., & Picard, B. (2013). Biological markers for meat tenderness of the three main French beef breeds using 2-DE and MS approach. In F. Toldrá, & L. M. L. Nollet (Eds.), *Proteomics in Foods: Principles and Application, Food Microbiology and Food Safety* (pp. 127-146). New York: Springer Science+Business Media.

Chen, L., Li, X., Ni, N., Liu, Y., Chen, L., Wang, Z., Shen, Q. W., & Zhang, D. (2016). Phosphorylation of myofibrillar proteins in post-mortem ovine muscle with different tenderness. *Journal of the Science of Food and Agriculture, 96*, 1474-83.

De Souza Rodrigues, R. T., Chizzotti, M. L., Vital, C. E., Baracat-Pereira, M. C., Barros, E., Busato K. C., Gomes, R. A., Ladeira, M. M., & da Silva Martins, T. (2017). Differences in beef quality between Angus (*Bos taurus taurus*) and Nellore (*Bos taurus indicus*) cattle through a proteomic and phosphoproteomic approach. *PloS One, 12 (1),* e0170294.

Efron, B. (1982). *The jacknife, the bootstrap and other resampling plans*. Philadelphia: Society for Industrial and Applied Mathematics, (Chapter 10).

548 FAO. The second report on the state of the world's animal genetic resources for food
549 and agriculture. (2015). http://www.fao.org/3/a-i4787e.pdf. Accessed 13.11.2019.
550 Fontanesi, L. (2017). Meat authenticity and traceability. In F. Toldra (Ed), *Lawrie´s*
551 *Meat Science* (pp. 585-633). England: Woodhead Publishing.
552 Franco, D., Mato, A., Salgado, F. J., López-Pedrouso, M., Carrera, M., Bravo, S.,
553 Parrado, M., Gallardo, J., & Zapata, C. (2015). Tackling proteome changes in the
554 *longissimus thoracis* bovine muscle in response to pre-slaughter stress. *Journal of*
555 *Proteomics*, *122*, 73-85.
556 Fu, H., Subramanian, R. R., & Masters, S. C. (2000). 14-3-3 proteins: structure,
557 function and regulation. *Annual Review of Pharmacology and Toxicology*, *40*, 617-
558 647.
559 Gagaoua, M., Terlouw, C., Richardson, I., Hocquette, J.-F., & Picard, B. (2019). The
560 associations between proteomic biomarkers and beef tenderness depend on the
561 end-point cooking temperature, the country origin of the panelists and breed. *Meat*
562 *Science*, *157*, 107871.
563 Graběz, V., Kathri, M., Phung, V., Moe, K. M., Slinde, E., Skaugen, M., Saarem, K., &
564 Egelandsdal, B. (2015). Protein expression and oxygen consumption rate of early
565 post-mortem mitochondria relate to meat tenderness. *Journal of Animal Science*,
566 *93*, 1967-1979.
567 Jaccard, P. (1908). Nouvelles recherches sur la distribution florale. *Bulletin de la*
568 *Société Vaudoise des Sciences Naturelles*, *44*, 223-270.
569 Lana, A., & Zolla L. (2016). Proteolysis in meat tenderization from the point of view of
570 each single protein: A proteomic perspective. *Journal of Proteomics*, *47*, 85-97.
571 López-Pedrouso, M., Bernal, J., Franco, D., & Zapata, C. (2014). Evaluating two-
572 dimensional electrophoresis profiles of the protein phaseolin as markers of genetic

differentiation and seed protein quality in common bean (*Phaseolus vulgaris* L.). *Journal of Agricultural and Food Chemistry*, *62*, 7200-7208.

López-Pedrouso, M., Pérez-Santaescolática, C., Franco, D., Fulladosa, E., Carvallo, J., Zapata, C., & Lorenzo, J. M. (2018). Comparative proteomic profiling of myofibrillar proteins in dry-cured ham with different proteolysis indices and adhesiveness. *Food Chemistry*, *244*, 238-245.

López-Pedrouso, M., Rodríguez-Vázquez, R., Purriños, L., Oliván, M., García-Torres, S., Sentandreu, M. A., Lorenzo, J. M., Zapata, C., & Franco, D. (2019). Sensory analysis of three Spanish breeds in different livestock production systems and pre-slaughter handling conditions. Unpublished results.

MAPAMA. Datos de las Denominaciones de Origen Protegidas (D.O.P.), Indicaciones Geográficas Protegidas (I.G.P.) y Especialidades Tradicionales Garantizadas (E.T.G.) de Productos Agroalimentarios. Secretaría General de Agricultura y Alimentación. (2018). http://www.mapama.gob.es/es/alimentacion/temas/calidad-agroalimentaria/informedop_igp_2016_ver4_tcm30-437834.pdf. Accessed 13-11-2019.

Marquès, K., Sarazin, B., Chané-Favre, L., Zivy, M., & Thiellement, H. (2001). Comparative proteomics to establish genetic relationships in the Brassicaceae family. *Proteomics*, *1*, 1457-1462.

Mato, A., Rodríguez-Vázquez, R., López-Pedrouso, M., Bravo, S., Franco, D., & Zapata, C. (2019). The first evidence of global meat phosphoproteome changes in response to pre-slaughter stress. *BMC Genomics*, *20*, 590.

Medeiros de Oliveira Silva, R., Bonvino Stafuzza, N., de Oliveira Fragomeni, B., Miguel Ferreira de Camargo, G., Matos Ceacero, T., Noely dos Santos Gonçalves Cyrillo, J., Baldi, F., Augusti Boligon, A., Zelotti Mercadante, M. E., Lino

598 Lourenco, D., Misztal, I., Galvao de Albuquerque, L. (2017). Genome-wide
599 association study for carcass traits in an experimental Nelore cattle population.
600 *PloS One, 12 (1),* e0169860.
601 Montowska, M., & Pospiech, E. (2012). Myosin light chain isoforms retain their
602 species-specific electrophoretic mobility after processing, which enables
603 differentiation between six species: 2DE analysis of minced meat and meat
604 products made from beef, pork and poultry. *Proteomics, 12,* 2879-2889.
605 Mouzo, D., López-Pedrouso, M., Bernal, J., García, L., Franco, D., & Zapata, C. (2018).
606 Association of patatin-based proteomic distances with potato (*Solanum tuberosum*
607 L.) quality traits. *Journal of Agricultural and Food Chemistry, 66,* 11864-11872.
608 Muroya, S., Ohnishi-Kameyama, M., Oe, M., Nakajima, I., Shibata, M., & Chikuni, K.
609 (2007). Double phosphorylation of the myosin regulatory light chain during rigor
610 mortis of bovine longissimus muscle. *Journal of Agriculture and Food Chemistry,*
611 *55,* 3998-4004.
612 Nei, M., Li, W. H. (1979). Mathematical model for studying genetic variation in terms
613 of restriction endonucleases. *Proceedings of the National Academy of Sciences of*
614 *the United States of America, 76,* 5269-5273.
615 Ohsaki, H., Okada, M., Sasazaki, S., Hinenoya, T., Sawa, T., Iwanaga, S., Tsuruta, H.,
616 Mukai, F., & Mannen, H. (2007). Proteomic comparison between Japanese Black
617 and Holstein cattle by two-dimensional gel electrophoresis and identification of
618 proteins. *Asian-Australasian Journal of Animal Sciences, 20,* 638-644.
619 Perkins, A., Nelson, K. J., Parsonage, D., Poole, L. B., & Karplus, P. A. (2015).
620 Peroxiredoxins: Guardians against oxidative stress and modulators of peroxide
621 signaling. *Trends in Biochemical Sciences, 40,* 435-445.

Picard, B., & Gagaoua, M. (2020). Meta-proteomics for the discovery of protein biomarkers of beef tenderness: An overview of integrated studies. *Food Research International*, *127*, 108739.

Ramayo-Caldas, Y., Renand, G., Ballester, M., Saintilan, R., & Rocha, D. (2016). Multi-breed and multi-trait co-association analysis of meat tenderness and other meat quality traits in three French cattle breeds. *Genetics Selection Evolution*, *48*, 37.

Rodríguez-Vázquez, R., & Zapata, C. (2019, September). A novel measure of quantitative proteomic distance. Poster session presentation at the 2nd Food Chemistry Conference, Sevilla, Spain.

Sentandreu, M. A., Fraser, P. D., Halket, J., Patel, R., & Bramley, M. (2010). A proteomic-based approach for detection of chicken in meat mixes. *Journal of Proteome Research*, *9*, 3374-3383.

Stull, J. T., Kamm, K. E., & Vandenboom, R. (2011). Myosin light chain kinase and the role of myosin light chain phosphorylation in skeletal muscle. *Archives of Biochemistry and Biophysics*, *510*, 120-128.

Szklarczyk, D., Gable, A. L., Lyon, D., Junge, A., Wyder, S., Huerta-Cepas, J., Simonovic, M., Doncheva, N. T., Morris, J. H., Bork, P., Jensen, L. J., & von Mering, C. (2019). STRING v11: protein-protein association networks with increased coverage, supporting functional discovery in genome-wide experimental datasets. *Nucleic Acids Research*, *47*, D607-613.

Telleria, J., Biron, D. G., Brizard, J.-P., Demettre, E., Séveno, M., Barnabé, C., Ayala, F. J., & Tibayrenc, M. (2010). Phylogenetic character mapping of proteomic diversity shows high correlation with subspecific phylogenetic diversity in

Trypanosoma cruzi. *Proceedings of the National Academy of Sciences of the United States of America*, *107*, 20411-20416.

Timperio, A. M., D'Alessandro, A.; Pariset, L., D'Amici, G. M., Valentini, A., & Zolla, L. (2009). Comparative proteomics and transcriptomics analyses of livers from two different *Bos taurus* breeds: "Chianina and Holstein Friesian". *Journal of Proteomics*, *73*, 309-322.

Wimmers, K., Murani, E., Te Pas, M. F. W., Chang, K. C., Davoli, R., Merks, J. W. M., Henne, H., Muraniova, M., da Costa, N., Harlizius, B., Schellander, K., Böll, I., Braglia, S., de Witt, A. A. C., Cagnazzo, M., Fontanesi, L., Prins, D., & Ponsuksili, S. (2007). Associations of functional candidate genes derived from gene-expression profiles of prenatal porcine muscle tissue with meat quality and muscle deposition. *Animal Genetics*, *38*, 474-484.

659 **Figure captions**

660 **Fig. 1.** Representative SYPRO Ruby-stained 2-DE gel images from LT meat samples of
661 different Spanish bovine breeds (AV, RE and RG). Differentially represented ($P < 0.05$)
662 protein spots between meat samples are marked and numbered.

663 **Fig. 2.** Heat map for normalized volume of protein spots with differential (*P*-value <
664 0.05) abundance between AV, RE and RG breeds. Green and red colors represent
665 relatively high and low values of protein abundance, respectively.

666 **Fig. 3.** UPGMA clustering dendrogram based on the matrix of pairwise differences in
667 *RC* (absolute values) of differentially ($P < 0.05$) changing proteins between AV-RG
668 (A), AV-RG (B) and RE-RG (C) bovine breeds.

669 **Fig. 4.** Protein-protein interaction network of differentially abundant proteins between
670 AV, RE and RG breeds, according to STRING confidence view (specific settings:
671 number of interactions to show, zero in the first and the second shell). The nodes
672 (circles) represent proteins and, the edges show known or predicted functional
673 associations (threshold: 0.4, medium confidence interval), and the colored lines indicate
674 the various types of interaction evidence (blue: co-occurrence; black: coexpression;
675 light blue: database evidence; green: neighborhood evidence; purple: experimental
676 evidence; red: fusion evidence; yellow: text mining evidence).

677 **Fig. 5.** Qualitative (Nei and Li's and Jaccard's *D*) and quantitative (*QD*) proteomic
678 distances between bovine breeds (AV, RE and RG) from meats of LT muscle.
679 Statistically significant differences ($P < 0.05$) between estimates of proteomic distance
680 assessed by 95% bootstrap confidence intervals are indicated with different lower case
681 letters (a and b).

Table 1

Differentially represented ($P < 0.05$) 2-DE protein spots between beef breeds (AV, RE and RG) identified by MALDI-TOF and MALDI-TOF/TOF MS.

Spot code[a]	Protein[b]	Abbrev.	Accession No. (Uniprot)	Mascot score	Sequence Cov. (%)	No. of matched peptides	p*I* (Th/ Obs)[c]	M_r (Th/ Obs) (kDa)[c]	Between-breed volume differences[d]
1	Myosin binding protein H	MYBPH	G3X6W9	147	18	7	5.82/ 5.56	53.6/ 72.5	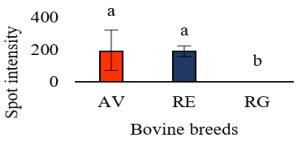
3	Myosin binding protein H	MYBPH-1	G3X6W9	181	20	8	5.82/ 6.07	53.6/ 72.5	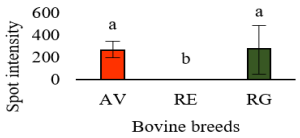
9	Creatine kinase M-type	CKM	Q9XSC6	60	11	5	6.63/ 6.60	43.2/ 45.6	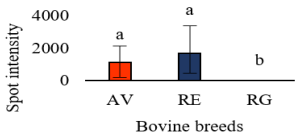
11	Thioredoxin-dependent peroxide reductase, mitochondrial	PRDX3	P35705	103	12	3	7.15/ 6.09	28.4/ 39.0	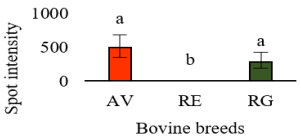

	precursor								
12	Actin alpha 1 skeletal muscle	ACTA1	P68138	83	12	5	5.23/ 6.11	42.3/ 41.6	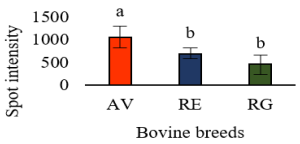
13	Pyruvate dehydrogenase E1 component subunit beta, mitochondrial	PDHB	P11966	67	43	7	5.39/ 5.39	39.4/ 38.5	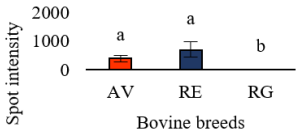
14	EGF domain-specific O-linked N-acetylglucosamine transferase	EOGT	A0JND3	51	11	8	6.87/ 6.11	**62.5/** **39.0**	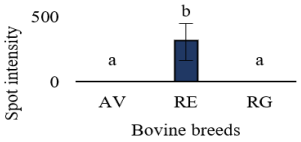
16	Pyruvate dehydrogenase E1 component subunit beta, mitochondrial	PDHB-1	P11966	67	27	10	6.21/ 5.44	39.4/ 38.0	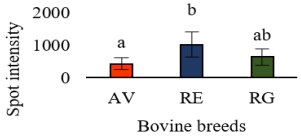

17	Troponin T, slow skeletal muscle	TNNT1	Q8MKH6	78	7	3	5.71/ 5.53	31.3/ 37.0	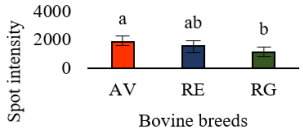
18	Actin, alpha skeletal muscle	ACTA1-1	P68138	87	12	5	5.23/ 4.71	42.4/ 33.0	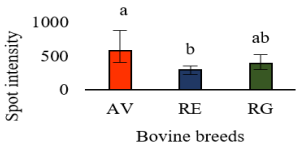
19	Ankyrin-2	ANK2	G3N0C1	64	9	27	8.15/ 5.51	25.8/ 31.5	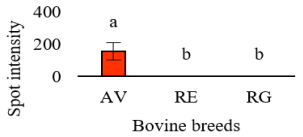
21	14-3-3 protein epsilon	YWHAE	P62261	63	10	3	4.63/ 4.25	29.3/ 27.5	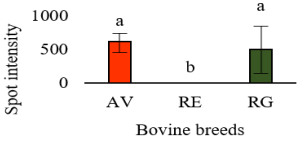
22	Cyclin-G1	CCNG1	Q5E9I1	61	13	8	9.21/ 4.95	34.6/ 27.1	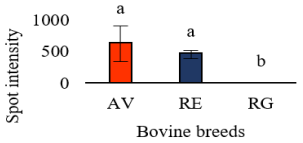

25	Myosin, light chain 6B, smooth, alkali, muscle and non-muscle	MYL6B	Q148H2	62	37	9	5.40/ 5.56	23.5/ 24.0	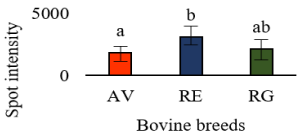
26	Thioredoxin-dependent peroxide reductase, mitochondrial	PRDX3-1	P35705	80	19	4	7.15/ 5.99	28.4/ 24.0	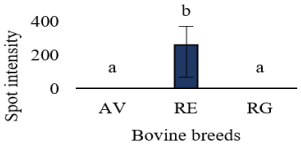
27	Transmembrane protein 233	TMEM223	A5PJW2	61	28	6	11.9/ 6.16	22.1/ 24.0	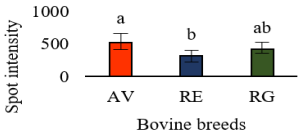
29	Myosin regulatory light chain 2, skeletal muscle isoform	MYLPF	Q0P571	150	47	8	4.91/ 4.25	19.1/ 19.1	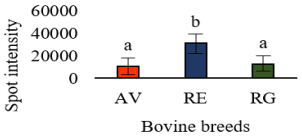
30	Myosin regulatory light chain 2, skeletal muscle isoform.	MYLPF-1	Q0P571	138	35	6	4.91/ 4.56	19.1/ 19.1	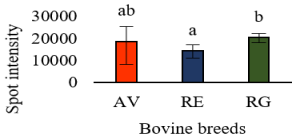

31	Myosin regulatory light chain 2, skeletal muscle isoform	MYLPF-2	Q0P571	140	48	8	4.91/ 4.56	19.1/ 19.1	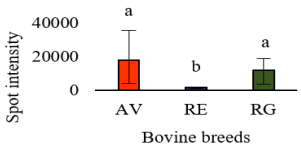
32	Protein FAM110A	FAM110A	Q58DG5	51	21	9	10.14/ 5.02	**31.8/ 16.3**	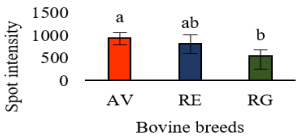
33	RNA/RNP complex-interacting phosphatase	DUSP11	Q5E999	53	35	9	9.32/ 5.94	**39.4/ 14.5**	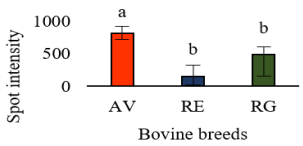
34	Protein FAM110A	FAM110A-1	Q58DG5	52	24	9	10.14/ 5.19	**31.8/ 12.0**	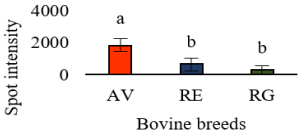
35	Ataxin-10	ATXN10	Q2TBW0	54	14	8	5.08/ 5.61	**53. 7/ 11.7**	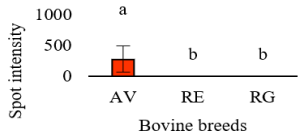

36	Branched-chain-amino-acid aminotransferase	BCAT2	Q5EA40	50	14	6	8.87/ 6.43	**45.0/ 12.5**	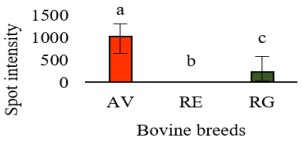
37	Spindle and kinetochore-associated protein 1	SKA1	Q0V7M7	53	46	10	6.77/ 4.99	**29.6/ 10.2**	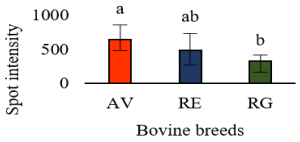

[a] Spot position is shown in Fig 1.

[b] Protein identifications matched to *B. taurus* protein databases.

[c] Theoretical (Th) p*I* and M_r values were obtained from UniProtKB/Swiss-Prot databases. Protein fragments [M_r (Th)/M_r (Obs) > 1.5] are denoted in bold.

[d] Mean volumes obtained from six biological replicates of each bovine breed together with their 95% CIs adjusted with the Bonferroni correction. Different lower-case letters indicate a significant difference ($P < 0.05$) in mean volume between bovine breeds.

Asturiana de los Valles Retinta Rubia Gallega

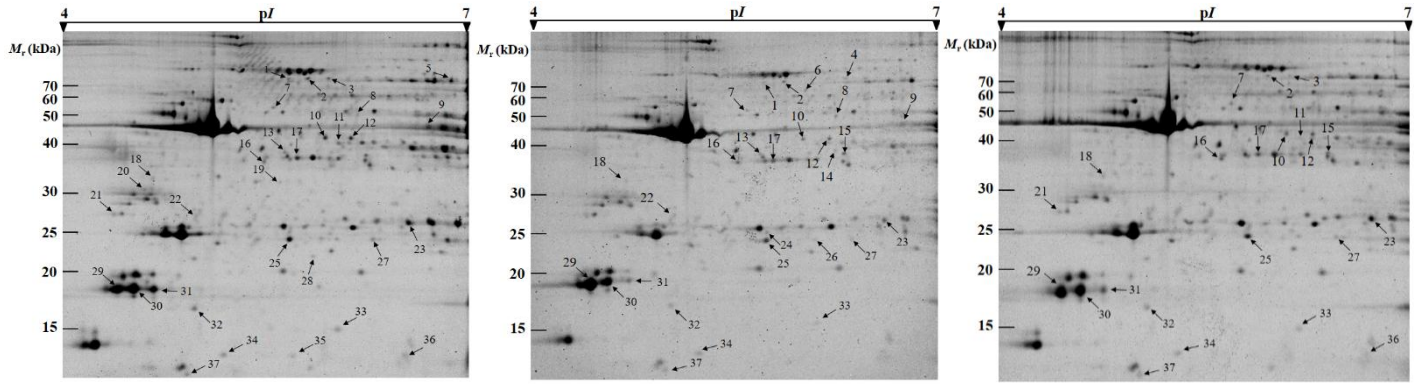

Fig. 1

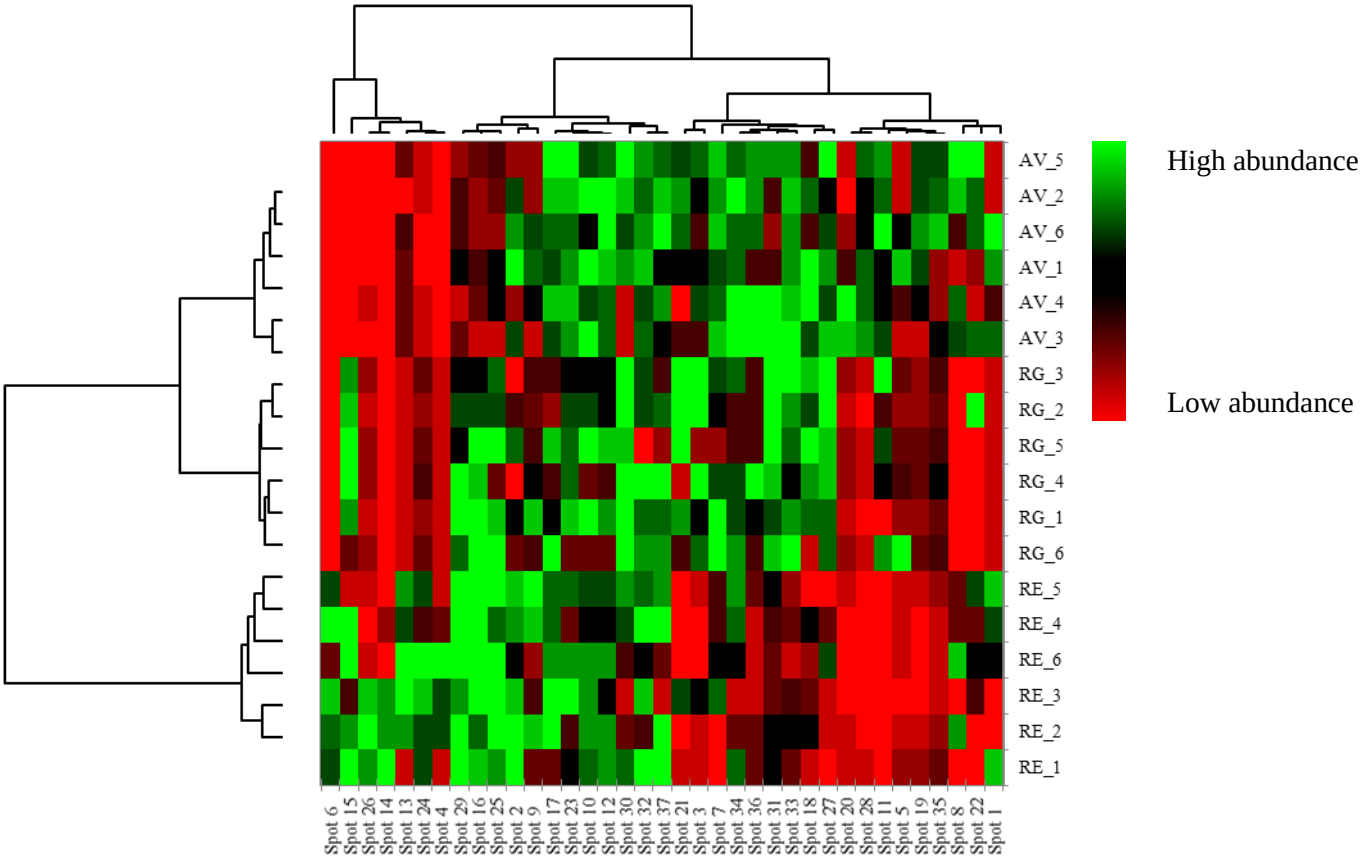
AV_5
AV_2
AV_6
AV_1
AV_4
AV_3
RG_3
RG_2
RG_5
RG_4
RG_1
RG_6
RE_5
RE_4
RE_6
RE_3
RE_2
RE_1
Spot 6
Spot 15
Spot 26
Spot 14
Spot 13
Spot 24
Spot 4
Spot 29
Spot 16
Spot 25
Spot 2
Spot 9
Spot 17
Spot 23
Spot 10
Spot 12
Spot 30
Spot 32
Spot 37
Spot 21
Spot 3
Spot 7
Spot 34
Spot 36
Spot 31
Spot 33
Spot 18
Spot 27
Spot 20
Spot 28
Spot 11
Spot 5
Spot 19
Spot 35
Spot 8
Spot 22
Spot 1
High abundance
Low abundance

Fig. 2

A)

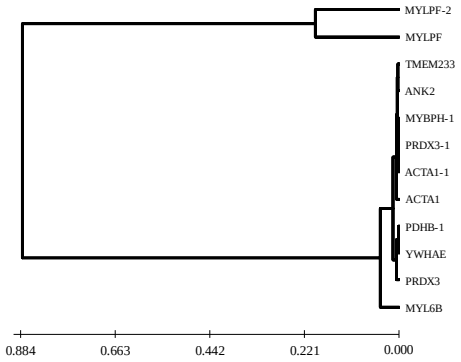

***RC* (absolute values) between AV-RE**

B)

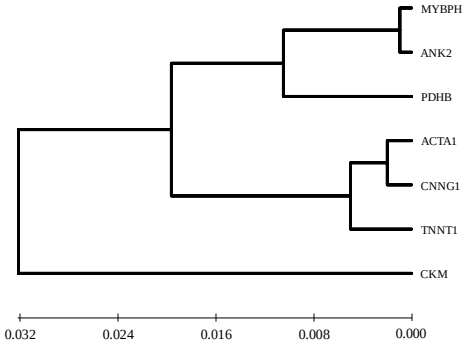

***RC* (absolute values) between AV-RG**

C)

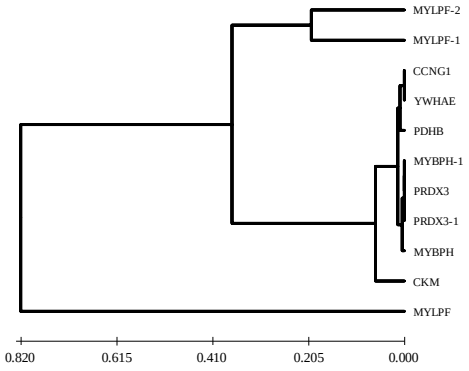

***RC* (absolute values) between RE-RG**

Fig. 3

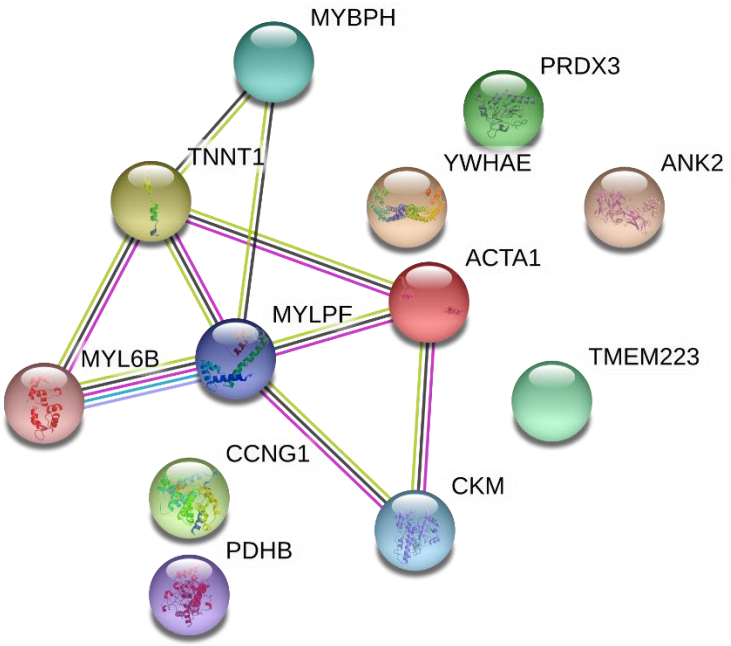
MYBPH
PRDX3
TNNT1
YWHAE
ANK2
ACTA1
MYLPF
MYL6B
TMEM223
CCNG1
CKM
PDHB

Fig. 4

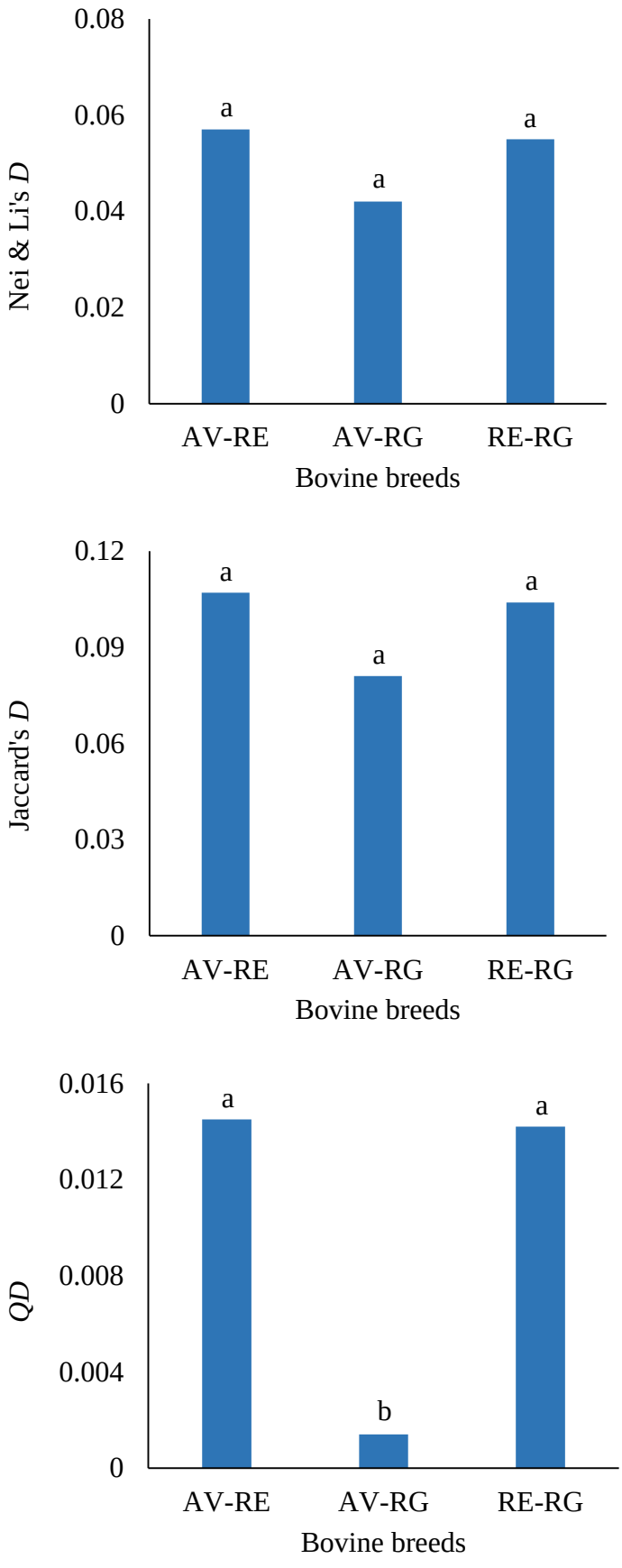
0.08
0.06
0.04
0.02
0
Nei & Li's D
a
a
a
AV-RE
AV-RG
RE-RG
Bovine breeds
0.12
0.09
0.06
0.03
0
Jaccard's D
a
a
a
AV-RE
AV-RG
RE-RG
Bovine breeds
0.016
0.012
0.008
0.004
0
QD
a
b
a
AV-RE
AV-RG
RE-RG
Bovine breeds

Fig. 5

Supplementary data

Measuring quantitative proteomic distance between Spanish beef breeds

R. Rodríguez-Vázquez, A. Mato, M. López-Pedrouso, D. Franco, M. A. Sentandreu, C. Zapata

Supplementary Tables 1-4

Supplementary Figures 1-3

Supplementary Table 1

Mean volume **(**± SE) and 95% CI interval for 2-DE spots with statistically significant differential abundance between Asturiana de los Valles (AV), Retinta (RE) and Rubia Gallega (RG**)** bovine meat samples from *longissimus thoracis* muscle.

Spot code[a]	AV		RE		RG		*P*-value[d]		
	Volume[b]	95% bootstrap CI (CL, CU)[c]	Volume[b]	95 % bootstrap CI (CL, CU)[c]	Volume[b]	95 % bootstrap CI (CL, CU)[c]	AV-RE	AV-RG	RE-RG
1	188 ± 47	69, 320	188 ± 13	152, 222	–	–	ns	< 0.05	< 0.05
2	354 ± 56	206, 499	412 ± 30	329, 499	208 ± 23	145, 279	ns	ns	< 0.05
3	262 ± 27	197, 342	–	–	278 ± 82	48, 482	< 0.05	ns	< 0.05
4	–	–	343 ± 67	203, 564	–	–	< 0.05	N/A	< 0.05
5	759 ± 223	191, 1426	–	–	–	–	< 0.05	< 0.05	N/A
6	–	–	181 ± 14	155, 227	–	–	< 0.05	N/A	< 0.05
7	343 ± 17	296, 388	247 ± 19	199, 295	229 ± 35	146, 328	< 0.05	ns	ns
8	430	262, 568	340 ± 51	224, 511	–	–	ns	< 0.05	< 0.05
9	1099 ± 369	183, 2111	1645 ± 527	463, 3357	–	–	ns	< 0.05	< 0.05
10	920 ± 90	703, 1123	661 ± 53	549, 824	464 ± 99	227, 707	ns	< 0.05	ns
11	497 ± 60	353, 684	–	–	284 ± 43	188, 421	< 0.05	ns	< 0.05
12	1041 ± 95	812, 1294	675 ± 49	578, 809	449 ± 86	226, 661	< 0.05	< 0.05	ns
13	390 ± 37	285, 493	679 ± 113	455, 989	–	–	ns	< 0.05	< 0.05
14	–	–	315 ± 51	162, 447	–	–	< 0.05	N/A	< 0.05

15	–	–	542 ± 96	208, 768	484 ± 60	308, 629	< 0.05	< 0.05	ns
16	420 ± 68	252, 602	1004 ± 137	633, 1411	646 ± 96	369, 881	< 0.05	ns	ns
17	1839 ± 115	1586, 2243	1521 ± 153	1059, 1917	1120 ± 133	813, 1464	ns	< 0.05	ns
18	573 ± 89	399, 873	286 ± 23	218, 344	386 ± 41	295, 513	< 0.05	ns	ns
19	155 ± 18	104, 208	–	–	–	–	< 0.05	< 0.05	N/A
20	855 ± 186	359, 1337	–	–	–	–	< 0.05	< 0.05	N/A
21	613 ± 54	440, 733	–	–	491 ± 131	134, 834	< 0.05	ns	< 0.05
22	633 ± 106	335, 901	473 ± 25	383, 518	–	–	ns	< 0.05	< 0.05
23	2805 ± 117	2495, 3189	1769 ± 330	1067, 2717	1316 ± 206	773, 1936	ns	< 0.05	ns
24	–	–	819 ± 215	419, 1361	–	–	< 0.05	N/A	< 0.05
25	1859 ± 213	1134, 2361	3111 ± 296	2448, 3980	2115 ± 297	1246, 2871	< 0.05	ns	ns
26	–	–	259 ± 55	67, 370	–	–	< 0.05	N/A	< 0.05
27	524 ± 46	417, 664	321 ± 35	227, 406	420 ± 29	359, 529	< 0.05	ns	ns
28	201 ± 12	165, 232	–	–	–	–	< 0.05	< 0.05	N/A
29	10643 ± 2720	3337, 18142	30974 ± 3253	21885, 38915	12258 ± 2516	6497, 19628	< 0.05	ns	< 0.05
30	18414 ± 3337	8176, 25263	14254 ± 1129	10849, 16897	20273 ± 725	18058, 22047	ns	ns	< 0.05
31	17907 ± 6060	4013, 35511	1561 ± 152	1138, 1946	11622 ± 3115	3655, 19059	< 0.05	ns	< 0.05
32	941 ± 53	784, 1057	804 ± 83	595, 1016	547 ± 95	256, 675	ns	< 0.05	ns
33	815 ± 38	717, 921	153 ± 57	20, 324	423 ± 88	151, 610	< 0.05	< 0.05	ns
34	1809 ± 151	1470, 2240	691 ± 146	211, 1020	283 ± 108	24, 551	< 0.05	< 0.05	ns
35	267 ± 75	69, 493	–	–	–	–	< 0.05	< 0.05	N/A

36	1023 ± 119	638, 1293	–	–	227 ± 101	28, 581	< 0. 05	< 0.05	< 0.05
37	637 ±72	472, 854	486 ± 84	265, 734	322 ± 51	158, 414	ns	< 0.05	ns

[a] Gel position of marked spots is shown in Fig.1.
[b] Mean volumes from six biological replicates.
[c] CI, Confidence interval; CL, lower bound; CU, upper bound; 95% bootstrap CIs were obtained by the bias-corrected percentile method and adjusted by the Bonferroni method for multiple comparisons.
[d] *P*-value < 0.05: statistically significant difference in mean volume between Spanish bovine breeds; ns: not statistically significant difference (*P* > 0.05); N/A: not applicable.

Supplementary Table 2

Fold change (*FC*) and relative change (*RC*) of differentially ($P < 0.05$) abundant proteins between Asturiana de los Valles (AV), Retinta (RE) and Rubia Gallega (RG) bovine meats from LT muscle.

Spot code[a]	Protein name (Abbrev.)	AV-RE		AV-RG		RE-RG	
		FC	*RC*	*FC*	*RC*	*FC*	*RC*
1	Myosin binding protein H (MYBPH)	ns	ns	-∞	-0.009	-∞	-0.009
3	Myosin binding protein H (MYBPH-1)	-∞	-0.013	ns	ns	+∞	+0.014
9	Creatine kinase M-type (CKM)	ns	ns	-∞	-0.054	-∞	-0.081
11	Thioredoxin-dependent peroxide reductase (PRDX3), mitochondrial precursor	-∞	-0.024	ns	ns	+∞	+0.014
12	Actin Alpha 1 skeletal muscle (ACTA1)	-1.54	-0.018	-2.33	-0.029	ns	ns
13	Pyruvate dehydrogenase E1 component subunit beta, mitochondrial (PDHB)	ns	ns	-∞	-0.019	-∞	-0.033
16	Pyruvate dehydrogenase E1 component subunit beta, mitochondrial (PDHB-1)	+2.39	+0.029	ns	ns	ns	ns
17	Troponin T, slow skeletal muscle (TNNT1)	ns	ns	-1.64	-0.035	ns	ns
18	Actin, alpha skeletal muscle (ACTA1-1)	-2.00	-0.014	ns	ns	ns	ns
19	Ankyrin-2 (ANK2)	+∞	-0.008	-∞	-0.008	N/A	N/A
21	14-3-3 protein epsilon (YWHAE)	-∞	-0.030	ns	ns	+∞	+0.024
22	Cyclin-G1 (CCNG1)	ns	ns	-∞	-0.031	-∞	-0.023
25	Myosin, light chain 6B, smooth muscle and non-muscle (MYL6B)	+1.67	+0.062	ns	ns	ns	ns
26	Thioredoxin-dependent peroxide reductase (PRDX3-1)	+∞	+0.013	N/A	N/A	-∞	-0.013

27	Transmembrane protein 233 (TMEM233)	-1.63	-0.010	ns	ns	ns	ns
29	Myosin regulatory light chain 2, skeletal muscle isoform (MYLPF)	+2.91	+1.000	ns	ns	-2.53	-0.921
30	Myosin regulatory light chain 2, skeletal muscle isoform (MYLPF-1)	ns	ns	ns	ns	+1.42	+0.296
31	Myosin regulatory light chain 2, skeletal muscle isoform (MYLPF-2)	-11.47	-0.804	ns	ns	+7.45	+0.495

[a] Gel position of marked spots is shown in Fig. 1.

ns: not statistically significant difference ($P > 0.05$).

N/A: not applicable.

Supplementary Table 3

Gene Ontology (GO) identifiers and terms (component, function and process) for differentially abundant proteins in LT meats from Asturiana de los Valles, Retinta and Rubia Gallega breeds obtained by the QuickGO tool.

Full protein name	Protein name	UniprotKB accession number	Ensembl gene accession number	GO Identifier and GO term name
Myosin binding protein H	MYBPH	G3X6W9	ENSBTAG00000011465	**Component**: GO:0005859 (muscle myosin complex), GO:0030018 (Z disc), GO:0031430 (M band) **Function**: GO:0008307 (structural constituent of muscle), GO:0051015 (actin filament binding), GO:0051371 (muscle alpha-actinin binding), GO:0097493 (structural molecule activity conferring elasticity) **Process**: GO:0006941 (striated muscle contraction), GO:0007015 (actin filament organization), GO:0045214 (sarcomere organization), GO:0071688 (striated muscle myosin thick filament assembly)
Creatine kinase M-type	CKM	Q9XSC6	ENSBTAG00000013921	**Component**: GO:0005615 (extracellular space), GO:0005737 (cytoplasm) **Function**: GO:0000166 (nucleotide binding), GO:0003824 (catalytic activity), GO:0004111 (creatine kinase activity), GO:0005524 (ATP binding), GO:0016301 (kinase activity), GO:0016740 (transferase activity), GO:0016772 (transferase activity, transferring phosphorus-containing groups) **Process**: GO:0009408 (response to heat), GO:0016310 (phosphorylation), GO:0046314 (phosphocreatine biosynthetic process)
Thioredoxin-dependent peroxide reductase, mitochondrial precursor	PRDX3	P35705	ENSBTAG00000008731	**Component**: GO:0005737 (cytoplasm), GO:0005739 (mitochondrion), GO:0005759 (mitochondrial matrix), GO:0005768 (endosome), GO:0005769 (early endosome), GO:0005829

				(cytosol), GO:0008385 (IkappaB kinase complex), GO:0043209 (myelin sheath), GO:0043234 (protein complex). **Function**: GO:0004601 (peroxidase activity), GO:0008022 (protein C-terminus binding), GO:0008379 (thioredoxin peroxidase activity), GO:0016209 (antioxidant activity), GO:0016491 (oxidoreductase activity), GO:0019900 (kinase binding), GO:0042802 (identical protein binding), GO:0043027 (cysteine-type endopeptidase inhibitor activity involved in apoptotic process), GO:0051920 (peroxiredoxin activity) **Process**: GO:0001893 (maternal placenta development), GO:0006915 (apoptotic process), GO:0006979 (response to oxidative stress), GO:0007005 (mitochondrion organization), GO:0008284 (positive regulation of cell proliferation), GO:0018171 (peptidyl-cysteine oxidation), GO:0030099 (myeloid cell differentiation), GO:0032496 (response to lipopolysaccharide), GO:0033673 (negative regulation of kinase activity), GO:0034599 (cellular response to oxidative stress), GO:0042542 (response to hydrogen peroxide), GO:0042744 (hydrogen peroxide catabolic process), GO:0043066 (negative regulation of apoptotic process), GO:0043154 (negative regulation of cysteine-type endopeptidase activity involved in apoptotic process), GO:0045454 (cell redox homeostasis), GO:0051092 (positive regulation of NF-kappaB transcription factor activity), GO:0051881 (regulation of mitochondrial membrane potential), GO:0055114 (oxidation-reduction process), GO:0098869 (cellular oxidant detoxification)
Actin, alpha skeletal muscle	ACTA1	P68138	ENSBTAG00000046332	**Component**: GO:0001725 (stress fiber), GO:0005737 (cytoplasm), GO:0005856 (cytoskeleton), GO:0005865 (striated muscle thin filament), GO:0005884 (actin filament), GO:0015629 (actin cytoskeleton), GO:0030017 (sarcomere), GO:0030027 (lamellipodium), GO:0030175 (filopodium), GO:0044297 (cell body) **Function**: GO:0000166 (nucleotide binding), GO:0005524 (ATP binding)

				Process: GO:0010628 (positive regulation of gene expression), GO:0030240 (skeletal muscle thin filament assembly), GO:0048741 (skeletal muscle fiber development), GO:0090131 (mesenchyme migration)
Pyruvate dehydrogenase E1 component subunit beta mitochondrial	PDHB	P11966	ENSBTAG00000021724	**Component**: GO:0005654 (nucleoplasm), GO:0005739 (mitochondrion), GO:0005759 (mitochondrial matrix), GO:0045254 (pyruvate dehydrogenase complex) **Function**: GO:0003824 (catalytic activity), GO:0004738 (pyruvate dehydrogenase activity), GO:0004739 (pyruvate dehydrogenase (acetyl-transferring) activity), GO:0016491 (oxidoreductase activity), GO:0034604 (pyruvate dehydrogenase (NAD+) activity) **Process**: GO:0005975 (carbohydrate metabolic process), GO:0006006 (glucose metabolic process), GO:0006086 (acetyl-CoA biosynthetic process from pyruvate), GO:0006099 (tricarboxylic acid cycle), GO:0008152 (metabolic process), GO:0055114 (oxidation-reduction process)
Troponin T, slow skeletal muscle	TNNT1	Q8MKH6	ENSBTAG00000006419	**Component**: GO:0005861 (troponin complex) **Function**: GO:0005523 (tropomyosin binding) **Process**: GO:0003009 (skeletal muscle contraction), GO:0006937 (regulation of muscle contraction), GO:0014883 (transition between fast and slow fiber), GO:0045932 (negative regulation of muscle contraction)
Ankyrin-2	ANK2	G3N0C1	ENSBTAG00000002392	**Component**: GO:0043034 (costamere) **Function**: GO:0030507 (spectrin binding) **Process**: GO:0007165 (signal transduction), GO:0098910 (regulation of atrial cardiac muscle cell action potential)

14-3-3 protein epsilon	YWHAE	P62261	ENSBTAG00000005664	**Component**: GO:0005634 (nucleus), GO:0005737 (cytoplasm), GO:0005739 (mitochondrion), GO:0005886 (plasma membrane), GO:0042470 (melanosome) **Function**: GO:0005246 (calcium channel regulator activity), GO:0015459 (potassium channel regulator activity), GO:0019899 (enzyme binding), GO:0019904 (protein domain specific binding), GO:0031625 (ubiquitin protein ligase binding); GO:0042802 (identical protein binding); GO:0042826 (histone deacetylase binding), GO:0044325 (ion channel binding), GO:0045296 (cadherin binding), GO:0046982 (protein heterodimerization activity), GO:0050815 (phosphoserine residue binding), GO:0051219 (phosphoprotein binding), GO:0097110 (scaffold protein binding) **Process**: GO:0000165 (MAPK cascade), GO:0001764 (neuron migration), GO:0006605 (protein targeting), GO:0021766 (hippocampus development), GO:0021987 (cerebral cortex development), GO:0034605 (cellular response to heat), GO:0035308 (negative regulation of protein dephosphorylation), GO:0046827 (positive regulation of protein export from nucleus), GO:0051480 (regulation of cytosolic calcium ion concentration), GO:0060306 (regulation of membrane repolarization), GO:1901016 (regulation of potassium ion transmembrane transporter activity), GO:1901020 (negative regulation of calcium ion transmembrane transporter activity), GO:1902309 (negative regulation of peptidyl-serine dephosphorylation), GO:1905913 (negative regulation of calcium ion export across plasma membrane)
Cyclin-G1	CCNG1	Q5E9I1	ENSBTAG00000006607	**Function**: GO:0005634 (nucleus) **Process**: GO:0007049 (cell cycle), GO:0051301 (cell division), GO:0051726 (regulation of cell cycle)
Myosin, light chain 6B, smooth, alkali, muscle	MYL6B	Q148H2	ENSBTAG00000031217	**Function**: GO:0005509 (calcium ion binding)

and non-muscle				
Transmembrane protein 233	TMEM223	A5PJW2	ENSBT AG00000009487	**Component**: GO:0005739 (mitochondrion), GO:0016020 (membrane), GO:0016021 (integral component of membrane) **Process**: GO:0007399 (nervous system development)
Myosin regulatory light chain 2, skeletal muscle isoform	MYLPF	Q0P571	ENSBTAG00000021218	**Component**: GO:0016459 (myosin complex) **Function**: GO:0005509 (calcium ion binding), GO:0008307 (structural constituent of muscle), GO:0046872 (metal ion binding) **Process**: GO:0007519 (skeletal muscle tissue development)

Supplementary Table 4

Estimates of qualitative and quantitative proteomic distances between Asturiana de los Valles (AV), Retinta (RE) and Rubia Gallega (RG) bovine breeds from meats of LT muscle.

Distance measure	AV-RE[a]	AV-RG[a]	RE-RG[a]
Nei & Li's *D*	0.057 (0.029, 0.102)	0.042 (0.019, 0.084)	0.055 (0.027, 0.097)
Jaccard's *D*	0.107 (0.057, 0.186)	0.081 (0.037, 0.156)	0.104 (0.052, 0.178)
QD	0.0145 (0.0020, 0.0383)	0.0014 (0.0007, 0.0019)	0.0142 (0.0023, 0.0340)

[a] 95% bootstrap CI are shown in parentheses.

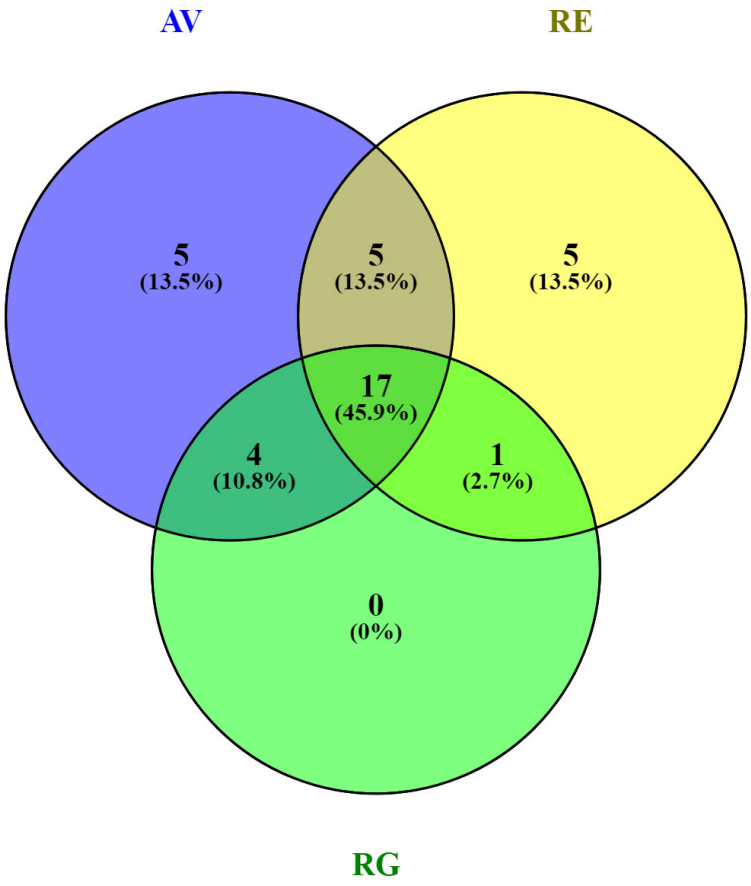

Supplementary Fig 1. Venn diagram showing the number (percentage) of shared and unshared differentially abundant protein spots from LT meat samples of the Asturiana de los Valles (AV), Retinta (RE) and Rubia Gallega (RG) bovine breeds.

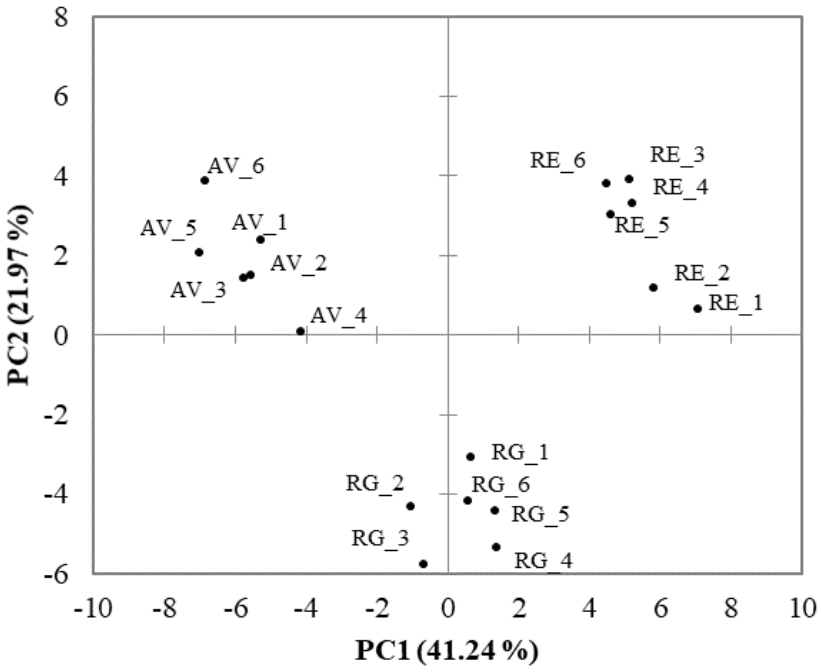

Supplementary Fig 2. PCA-plot for the first two principal components from standardized volume of protein spots with differential ($P < 0.05$) abundance between among bovine breeds (AV: Asturiana de los Valles; RE: Retinta; RG: Rubia Gallega).

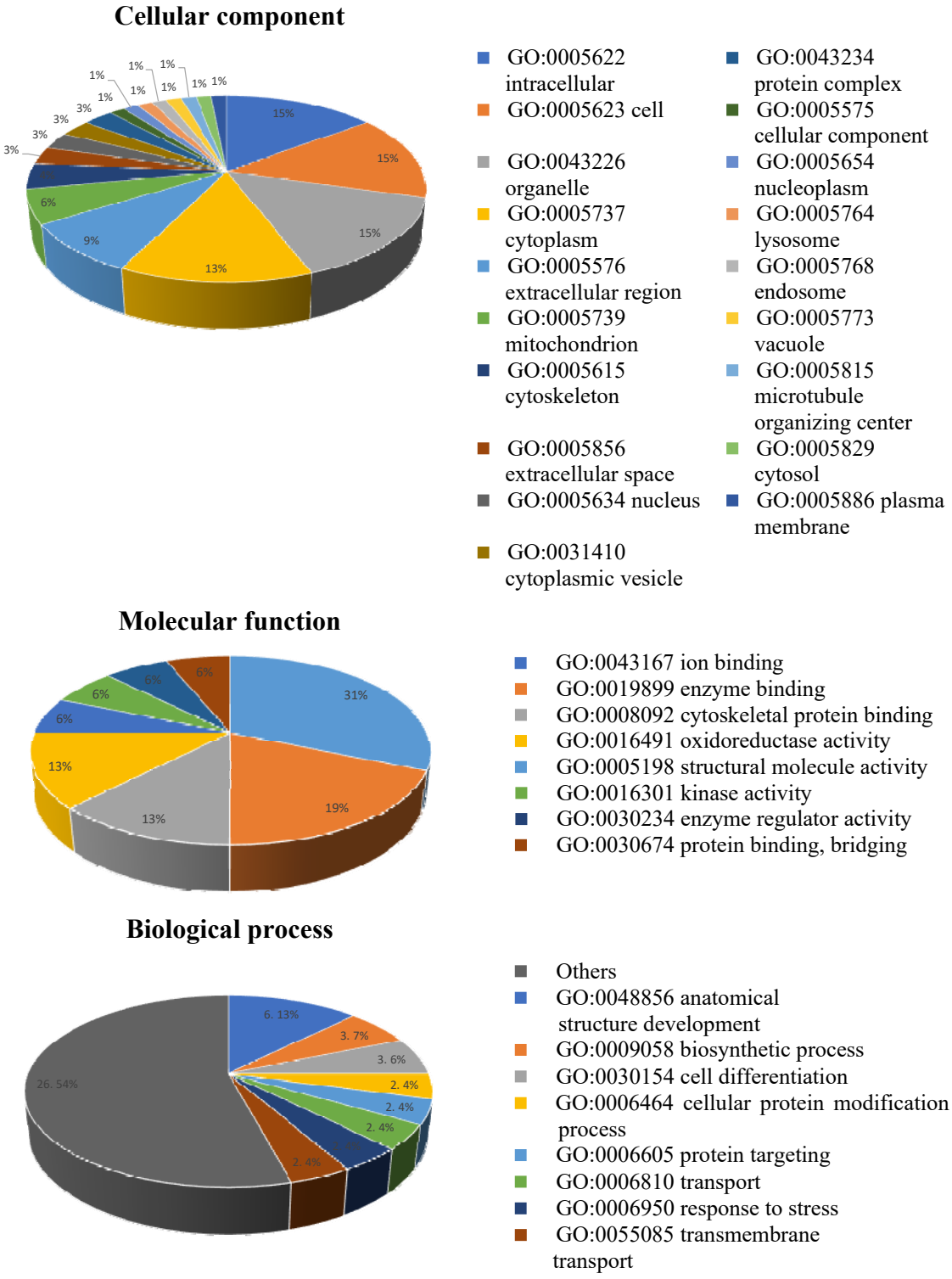

Supplementary Fig 3. Distribution of high level Gene Ontology (GO slim terms) in the three different ontologies (cellular component, molecular function and biological process) for the 12 differentially abundant proteins between LT meats of Asturiana de los Valles, Retinta and Rubia Gallega bovine breeds retrieved by means of the Slimmer tool of AmiGO software (http://amigo1.geneontology.org/cgi-bin/amigo/slimmer).